Surface Electronic Structure of Si(111)-(7×7) Resolved in Real Space

R. J. Hamers, R. M. Tromp, and J. E. Demuth
IBM Thomas J. Watson Research Center, Yorktown Heights, New York 10598
(Received 20 February 1986)

We have obtained the first energy-resolved real-space images of the filled and empty surface states of the Si(111)-(7×7) surface, with 3-Å lateral resolution. This ability to resolve spatially these surface states with a scanning tunneling microscope depends upon a new method to acquire and separate geometric and electronic information. Our results not only are in good agreement with previous spectroscopic studies but also directly reveal the atomic location and geometric origin of the Si(111)-(7×7) surface states.

PACS numbers: 73.20.Cw, 61.16.Di, 68.35.Bs, 73.40.Gk

Surface states play an important role in the physical properties of solid surfaces and have been the subject of numerous theoretical and experimental studies. While these states have been extensively studied in reciprocal space, real-space observation and determination of the geometric origins of surface states have hitherto not been possible. We have atomically resolved and directly identified the physical origin and nature of the various surface states of the Si(111)-(7×7) surface found in previous photoemission and inverse-photoemission studies. These include surface states due to dangling bonds on the twelve adatoms, several states localized on the atoms in the layer beneath the adatoms, a state due to Si—Si backbonds, and a state localized in the deep corner hole of the Si(111)-(7×7) surface. *In effect, we have mapped out the electronic states of the Si(111)-(7×7) surface with a lateral resolution of 3 Å.*

The utilization of scanning tunneling microscopy (STM) to probe surface electronic structure in real space has been plagued by a number of experimental problems.[1] In one reported approach,[2-4] I vs V or dI/dV vs V curves are measured without scanning. While such curves contain electronic structure information, the lateral position of the tip is uncertain and real-space images of the surface states are not obtained. Alternatively, images of dI/dV may be acquired at various bias voltages.[4] However, at each voltage the tip follows a different contour[5] so that the dI/dV images contain a mixture of geometric and electronic structure information, complicating interpretation of the observed features.[6] Ideally, one would like to know the complete I-V characteristics, at constant sample-tip separation, at each point in a topographic image.

Here we describe a new method, current-imaging-tunneling spectroscopy (CITS), which overcomes the problems inherent in the aforementioned techniques and allows real-space imaging of surface electronic states. In this method the feedback control circuit used for constant-current STM is gated so that it is only active about 30% of the time. When the feedback loop is active, a constant voltage is applied to the sample; when inactive, the position of the tip is held stationary and the tunneling current is measured at various different bias voltages. By the repeating of this sequence at 2.2 kHz a constant sample-tip separation is maintained during all I-V measurements and the I-V characteristics of each point along the raster scan are determined simultaneously with the topography. We have obtained current images at sample voltages between −2.5 and +2.5 V with the feedback loop stabilized at a sample voltage of +2.0 V and a tunneling current of 5.0 nA. This particular feedback voltage is specifically chosen to that the tip closely follows the atomic corrugations.[5] Then, the resulting real-space images of the tunneling current directly reflect the spatial distribution of the surface states without interference from geometric structure contributions.

The design of our microscope and the cleaning procedure of our samples (6 mΩ cm, Sb-doped) have been described previously.[7] Results have been reproduced with several samples and several tungsten tips. In Fig. 1 we show a constant-current topograph [Fig. 1(a)] and current images acquired *simultaneously* with voltages of +1.45 V [Fig. 1(b)] and −1.45 V [Fig. 1(c)] applied to the sample. In the topograph, protrusions are white and depressions are black with a total gray-scale range of 2 Å. In the current images, regions of high current are white and regions of low current are black. In Fig. 1(a) one (7×7) unit cell has been outlined, and the two halves have been identified as "faulted" (F) or "unfaulted" (U) in accordance with the dimer-adatom-stacking fault model of Takayanagi *et al.*[8] As previously noted[4] the positive-bias tunneling current image, Fig. 1(b), has a pronounced asymmetry with the unfaulted half of the cell giving rise to more current than the faulted half. The negative-bias current image, Fig. 1(c), has six points of high current centered between the adatoms while the rest of the unit cell appears to be rather uniform. These images show distinct bias-dependent structures that are derived from tunneling through all states lying between the Fermi levels of the tip and sample.[9] To identify the energies of these states, we first examine the I-V characteristics of the (7×7) surface.

Figure 2(a) shows conductance-voltage (σ-V) curves for the Si(111)-(7×7) surface when averaged

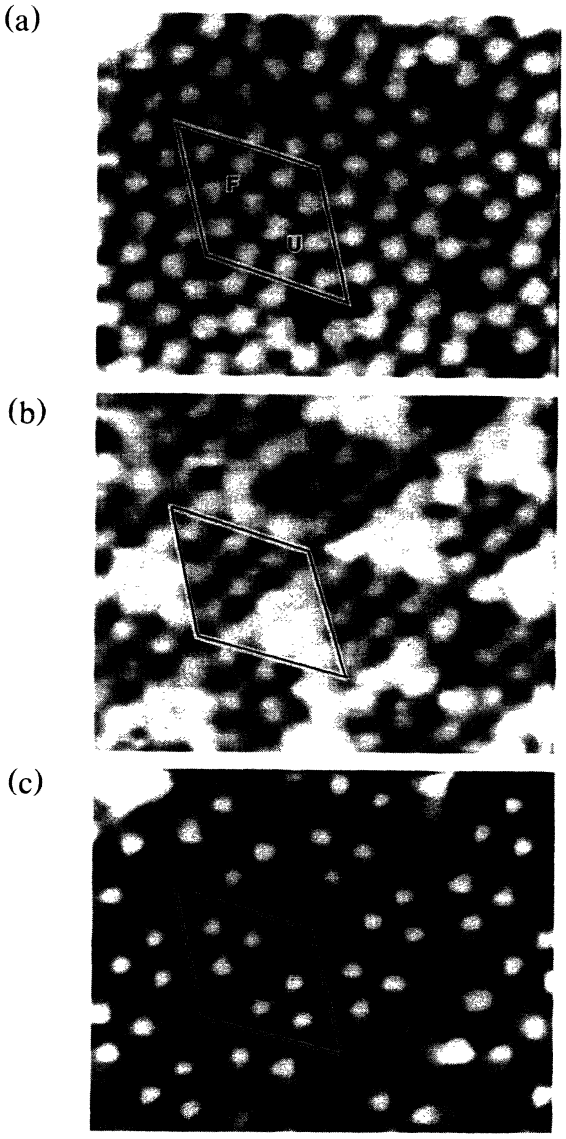

FIG. 1. Simultaneously acquired topograph and current images: (a) STM topograph with +2 V applied to the sample, and current images with (b) +1.45 V and (c) −1.45 V applied to the sample.

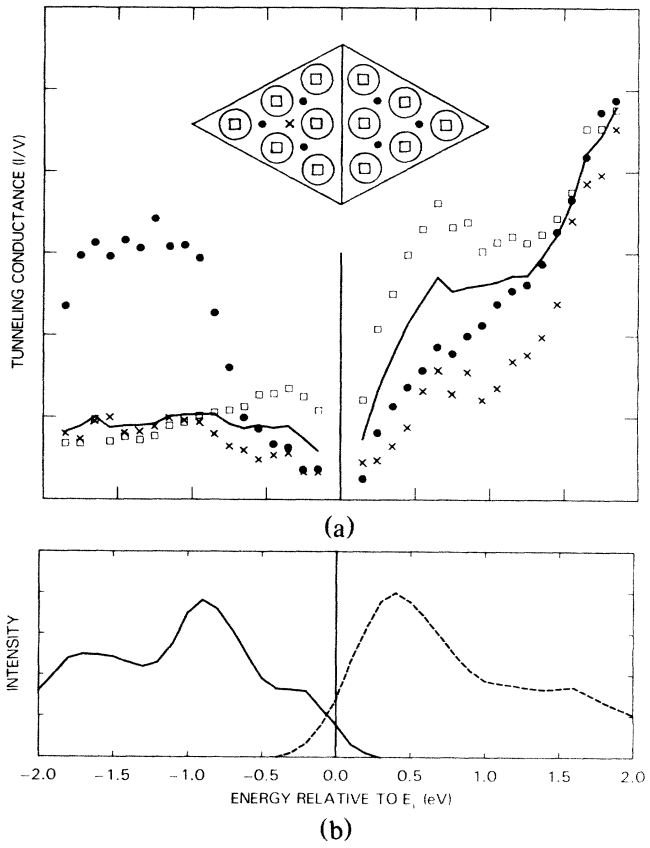

FIG. 2. (a) Constant-distance σ-V spectra for the Si(111)-(7×7) surface averaged over one unit cell (solid line) and at selected locations in the unit cell (other symbols). Crosses are from faulted half only; others are averaged over both halves of unit cell. (b) Surface observed using UPS (solid line) and IPS (dashed line), from Refs. 10 and 12.

over a single unit cell and also for some selected 2-Å-diam regions within the (7×7) unit cell. Upon a change in bias voltage the introduction of a surface state into the energy range between the Fermi levels of tip and sample opens a new channel for conduction and should produce a step, or onset, in the σ-V curve. In the spatially averaged σ-V curve (solid line) only small increases are observed near −1.7, −0.8, −0.4, +0.5, and +1.3 V. Much more dramatic conductance changes are observed in the σ-V profiles measured at specific points within the unit cell. For example, the increase observed near −0.8 V is almost completely localized in six 3-Å-diam regions *between* the adatoms, where the tunneling current increases by a factor of 5 (circles in Fig. 2). Similarly, the onsets at −0.2 and +0.5 V are localized on the adatoms (squares in Fig. 2), the onset near +1.3 V can be found where the layer beneath the adatoms is exposed to the vacuum (crosses in Fig. 2), and the small onset near −1.7 V is most pronounced near the deep corner holes of the (7×7) superlattice (not shown). The strong spatial dependence of the conductance observed here emphasizes the necessity of precise knowledge and control of the tip position during such measurements. From these spatially resolved σ-V curves we can clearly identify the energies of the surface states and directly relate them to the states observed in ultraviolet photoemission spectroscopy (UPS)[10,11] and inverse photoemission spectroscopy (IPS)[11,12] studies, shown in Fig. 2(b). The overall agreement between the onsets in the σ-V curves and the photoemission peaks is strong evidence that we are detecting the same surface states of the *sample*. Surprisingly, the electronic struc-

ture of the tip appears to be relatively unimportant.

In contrast to UPS and IPS, we are able to directly image these states in real space with a lateral resolution of 3 Å. In order to do so, we show in Fig. 3 the current difference between pairs of bias voltages above and below the onset voltages observed in the σ-V curves. At voltages between -0.15 and -0.65 V [Fig. 3(a)] most of the tunneling current arises from the dangling-bond states on the twelve adatoms. More current arises from adatoms in the faulted half of the unit cell than in the unfaulted half, and in both halves of the cell more current comes from the three adatoms adjacent to a corner hole than from the other three. We also find a nearly identical image at the lowest positive bias, $+0.15$ V. We cannot probe states exactly at E_F, but the similarity between images at the smallest positive and negative bias voltages suggests that they involve tunneling through the same metallic state, in agreement with UPS,[10,11] IPS,[11,12] and energy-loss studies.[13] This is the only state which at negative sample bias exhibits an asymmetry of the two halves of the unit cell and is thereby responsible for the asymmetry in the STM topographs of Binnig *et al.*[14] and of Tromp, Hamers, and Demuth.[5]

A differential current image between -1.0- and -0.6-V bias [Fig. 3(b)] shows three regions of high current between the six adatoms in each half of the unit cell exactly where the dimer-adatom-stacking model[8] has dangling bonds on the atoms in the layer beneath the adatoms. When our microscope has its highest lateral resolution we also observe a seventh high-current spike in the center of the corner holes, as in Fig. 3(b). This first observation of such dangling-bond states *not* associated with adatoms has important consequences for (7×7) structural models. For example, the reflection symmetry exhibited by these dangling bonds with respect to the short diagonal of the unit cell implies reflection symmetry in the atomic layer beneath the adatoms and directly indicates the presence of a stacking fault in one half of the unit cell.

Another occupied state with an onset at -1.7 V can be imaged as the differential current between -2.0 and -1.6 V. As shown in Fig. 3(c), this state is observed as regions of higher current density surrounding the adatoms where Si—Si backbonds are expected[15] and also as a diffuse circular patch at the corner hole where additional backbonds are exposed to the vacuum. Because of the spatial diffuseness of this state, the onset in the σ-V curves is most noticeable when measured near the corner hole. Tunneling from the corner hole at this energy is only weakly dependent on the sharpness of the tip and is qualitatively different from the tunneling though the bottom dangling bond sometimes observed at lower voltages. We find it rather remarkable that we are able to directly observe the Si—Si backbonds at all, since these tend to be localized in the surface plane. This spatial distribution demonstrates that the state observed at -1.75 eV in photoemission[10] is a backbond state[16] and not a dangling-bond state as has been suggested.[11]

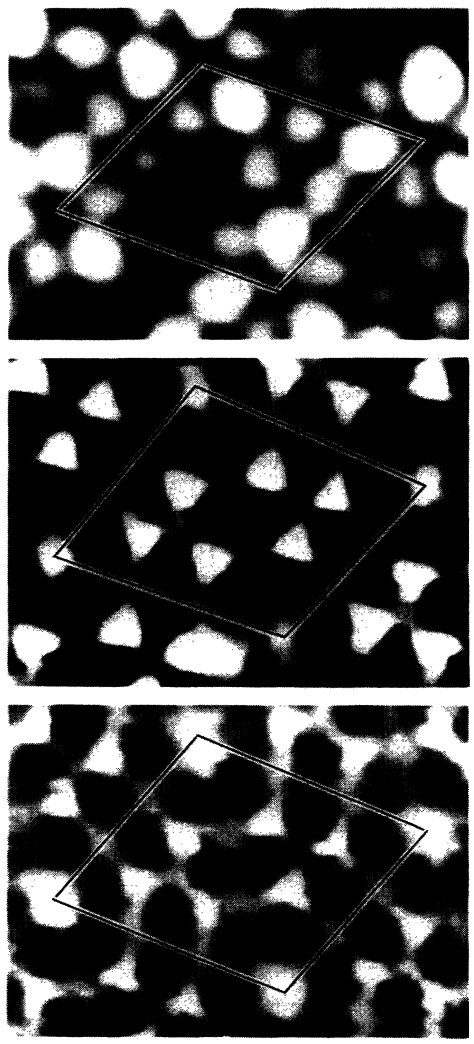

FIG. 3. CITS images of occupied Si(111)-(7×7) surface states. (a) Adatom state at -0.35 V, (b) dangling-bond state at -0.8 V, (c) backbond state at -1.7 V.

We have also identified and imaged the empty surface states of Si(111)-(7×7). In addition to the adatom state near E_F discussed earlier, another adatom state is observed near 0.5-V bias causing the large onset observed in the σ-V curves at this voltage. This state (not shown) has the tunneling current evenly distributed on all twelve adatoms making the unit cell appear symmetric at bias voltages between $+0.25$ and $+0.65$ V.

Two closely related states are observed near $+1.3$ V, localized between the adatoms where atoms in the layer beneath the adatoms and adatom backbonds are exposed to the vacuum. There is a pronounced differ-

ence between the onset voltages of these states in the faulted (1.4 V) and unfaulted (1.2 V) halves of the unit cell which shows that these states are intimately associated with the stacking sequence. This difference in onset voltages gives rise to asymmetry in STM topographs at positive bias voltage which has a sense opposite to that observed at negative bias.

In summary, we have presented the first energy-resolved real-space observations of surface states. We have identified both the filled and empty surface states of the Si(111)-(7×7) surface with atomic resolution and have established their geometric origins. These states are observed to be localized to regions as small as 3 Å in diameter. In contrast to other STM spectroscopic techniques the CITS technique introduced here allows a direct identification of surface electronic and geometric structure and greatly enhances the utility of the STM as a spectroscopic tool.

The authors thank Peter Schroer for his assistance in developing the data acquisition software and hardware. This work was supported in part by the U.S. Office of Naval Research.

[1]A. L. Robinson, Science **229**, 1074 (1985), and references therein.

[2]G. Binnig, K. H. Frank, H. Fuchs, N. Garcia, B. Reihl, and H. Rohrer, F. Salvan, and A. R. Williams, Phys. Rev. Lett. **50**, 991 (1985).

[3]R. M. Feenstra, W. A. Thompson, and A. P. Fein, Phys. Rev. Lett. **56**, 608 (1986).

[4]R. S. Becker, J. A. Golovchenko, D. R. Hamann, and B. S. Swartzentruber, Phys. Rev. Lett. **55**, 2032 (1985).

[5]R. M. Tromp, R. J. Hamers, and J. E. Demuth, to be published.

[6]A. Baratoff, Physica (Amsterdam) **127B+C**, 137 (1984).

[7]J. E. Demuth, R. J. Hamers, R. M. Tromp, and M. E. Welland, to be published.

[8]K. Takayanagi, Y. Tanishiro, M. Takahashi, and S. Takahashi, J. Vac. Sci. Technol. A **3**, 1502 (1985).

[9]J. Tersoff and D. R. Hamann, Phys. Rev. B **31**, 805 (1985).

[10]F. J. Himpsel and Th. Fauster, J. Vac. Sci. Technol. A **2**, 815 (1984).

[11]R. I. G. Uhrberg, G. V. Hansson, J. M. Nicholls, P. E. S. Persson, and S. A. Flodstrum, Phys. Rev. B **31**, 3805 (1985).

[12]Th. Fauster and F. J. Himpsel, J. Vac. Sci. Technol. A **1**, 1111 (1983).

[13]U. Backes and H. Ibach, Solid State Commun. **40**, 575 (1981).

[14]G. Binnig, H. Rohrer, Ch. Gerber, and E. Weibel, Phys. Rev. Lett. **50**, 120 (1983).

[15]J. E. Northrup, Phys. Rev. Lett. **53**, 683 (1984).

[16]J. A. Appelbaum and D. R. Hamann, Phys. Rev. Lett. **31**, 106 (1973).

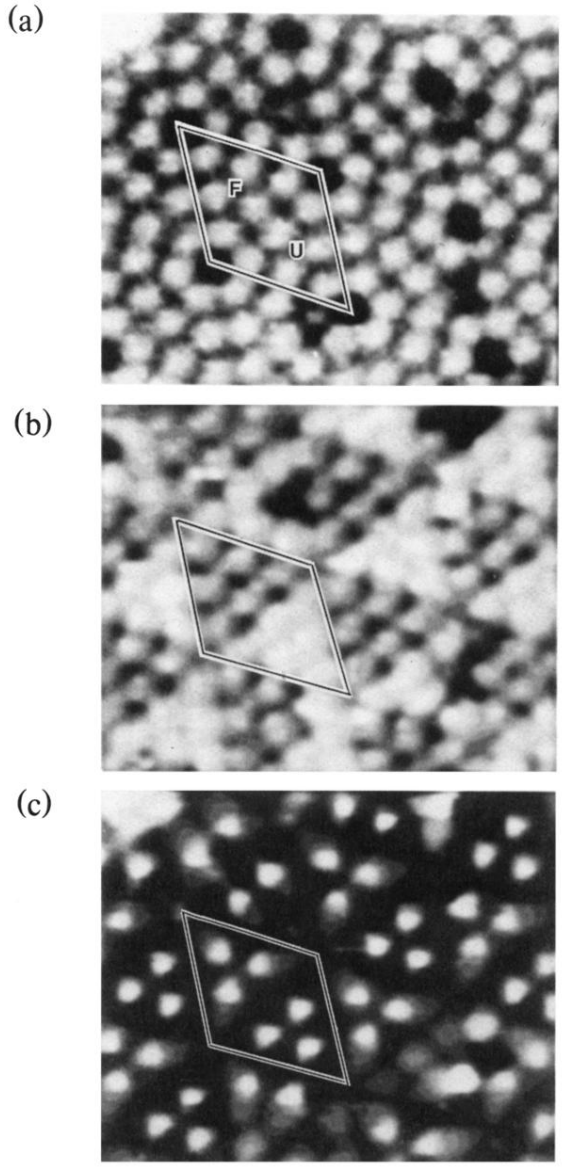

FIG. 1. Simultaneously acquired topograph and current images: (a) STM topograph with +2 V applied to the sample, and current images with (b) +1.45 V and (c) −1.45 V applied to the sample.

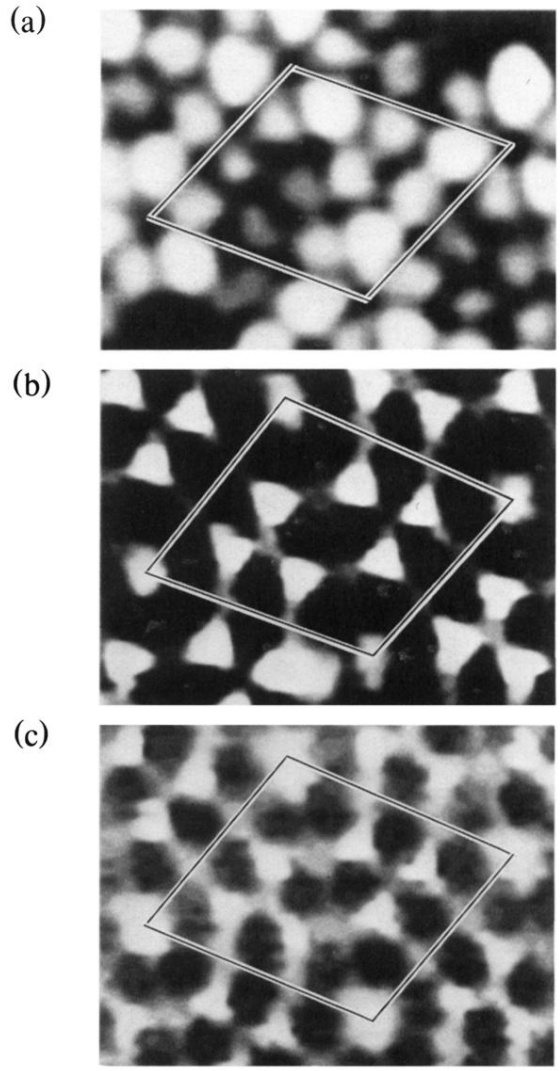

FIG. 3. CITS images of occupied Si(111)-(7×7) surface states. (a) Adatom state at −0.35 V, (b) dangling-bond state at −0.8 V, (c) backbond state at −1.7 V.